Spectrum of Engineering Sciences
ISSN (e) 3007-3138 (p) 3007-312X Volume 4, Issue 1, 2026

DESIGN AND EXPERIMENTAL EVALUATION OF A SOLAR ASSISTED ELECTRIC VEHICLE PROTOTYPE

Umar Nawaz[1], Haroon Akhtar[*2], M. Aftab Khan[3], M. Shahab Khan[4], M. Ahtesham-ul-Haq[5], Salman Khan Raziq[6], Muhammad Zia[7], Irshad Ullah[8]

*[1,*2,3,4,5,6]Department of Mechanical Engineering Technology, Shuhada-e-APS University of Technology, Nowshera*
[7,8]Department of Energy Engineering Technology, Shuhada-e-APS University of Technology, Nowshera

[*2]haroon@uotnowshera.edu.pk

DOI: https://doi.org/10.5281/zenodo.18207762

Keywords
electric vehicle, DC motor, lead acid battery, PWM charging, suspension, steering, aerodynamic shaping, speed, charging performance.

Article History
Received: 19 November 2025
Accepted: 26 December 2025
Published: 10 January 2026

Corresponding Author: *
Haroon Akhtar

Abstract
The rising fuel prices and pollution posed by the traditional vehicles have spawned an urgent demand of sustainable and affordable forms of transport. Furthermore, the utilization of non-renewable sources of energy limits the efficiency, availability, and long-term viability of vehicles, which highlights the need to create renewable energy-powered vehicles. This paper presents the design, fabrication, and experimental analysis of a miniature solar assisted electric vehicle (EV) prototype which is intended to be deployed in the low-speed urban mobility. The vehicle embeds a 1 kW DC motor, a 48 V lead acid battery pack, a PWM based charging system and a basic voltage-based battery protection system. The mechanical subsystems are a lightweight steel frame, independent suspension, rack and pinion steering and simple aerodynamic shaping. The operating conditions were set and experimental testing was run to measure the speed, range, and charging performance. The prototype was aimed at reaching 28 km per hour and 20 km solar assisted driving range. The findings indicate the feasibility of low-cost solar assisted electric vehicles in educational, research and localized transport modes of transportation.

INTRODUCTION

The transport industry is one of the biggest areas of energy expenditure and greenhouse gas emissions [1-5]. Recent studies suggest that the transport sector contributes to about 24 percent of direct CO_2 emissions due to the combustion of fuels [6-7]. EVs provide a viable solution in achieving a reduction in emissions, especially when applied in short-range and low-speed scenarios [7-8]. Nevertheless, in most of the developing world, the use of traditional EVs is limited by the availability of charging infrastructure, grid stability, and affordability [9-10].

One of the solutions is solar assisted EVs which combines onboard energy storage with direct photovoltaic charging. Solar power fills the gaps of grid charging in such systems and also lowers the reliance on external power sources. This is particularly applicable to low-speed vehicles whose energy requirements are small and working conditions are predictable [11-14].

The majority of the available literature on solar powered vehicles concentrates on advanced power electronics, optimization algorithms and high efficiency photovoltaic integration [15-20] . Though these studies are important, applied engineering work is required as well, where

complete system-level design, fabrication, and experimental testing are documented using readily available components. These studies find applications in academic laboratories, preliminary development, and in education programs.

This paper describes the design and experimental test of a mini solar supported EV prototype, designed to operate at low speed in an urban environment. The EV incorporates a 1 kW DC motor, a 48 V lead acid battery pack, a PWM based charging system and a simple voltage-based battery protection system. Mechanical systems such as the chassis, suspension, steering and braking were built to facilitate low speed stable operations.

This study aims to show the effective applicability of the incorporation of electrical, mechanical, and control subsystems into an efficient solar assisted electric vehicle. Speed, driving range, and charging performance are tested under controlled conditions of experimental testing.

The rest of the paper is structured in the following way. Section 2 describes design of electrical system and battery safety control. Section 3 provides the detailed mechanical design and aerodynamic considerations. Calculations and supporting system parameters are summarized in section 4. Section 5 provides the discussion of the experimental results and performance evaluation. Section 6 is the conclusion of the paper and presents the improvements to be made in the future.

2. System Design

2.1 Electrical Power Distribution

The electrical power architecture consists of high-voltage drive circuits and low-voltage support systems. These components are all interconnected in a comprehensive manner as depicted in the wiring schematics in Figure 1a and Figure 1b.

2.1.1 High-Voltage Traction Power System: This main loop is responsible to manages the EV drive energy. This portion consists of a 1 kW DC motor with series winding (48 V, 12 A nominal) and a 4-kWh large-capacity battery module (four 12 V, 70 Ah units in series). To mitigate high-current transients, the system incorporates a motor controller rated at 30 A, a main magnetic contactor rated 30–60 A, and an overcurrent protection breaker equipped with a 50–150 A trip range. The current flow within the system is precisely measured via the precision current shunts.

2.1.2 The Low-Voltage Auxiliary System: A 60 V to 12 V DC to DC converter electrically isolates the system of the traction loop. It provides electricity to indicators and warning devices. The operator operates the system by a master key switch and an accelerator pedal that has a potentiometer.

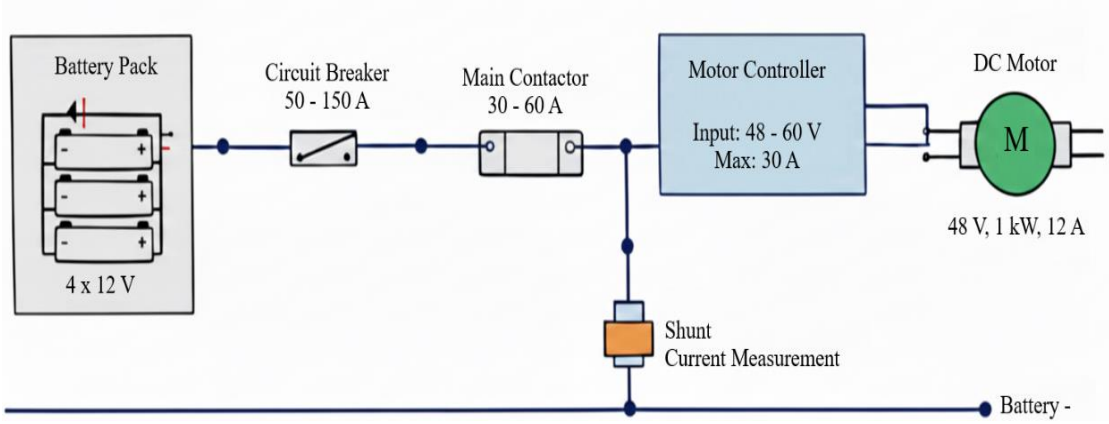

Figure 1a. Schematic of Complete Electric Wiring of the EV with High Voltage Power System.

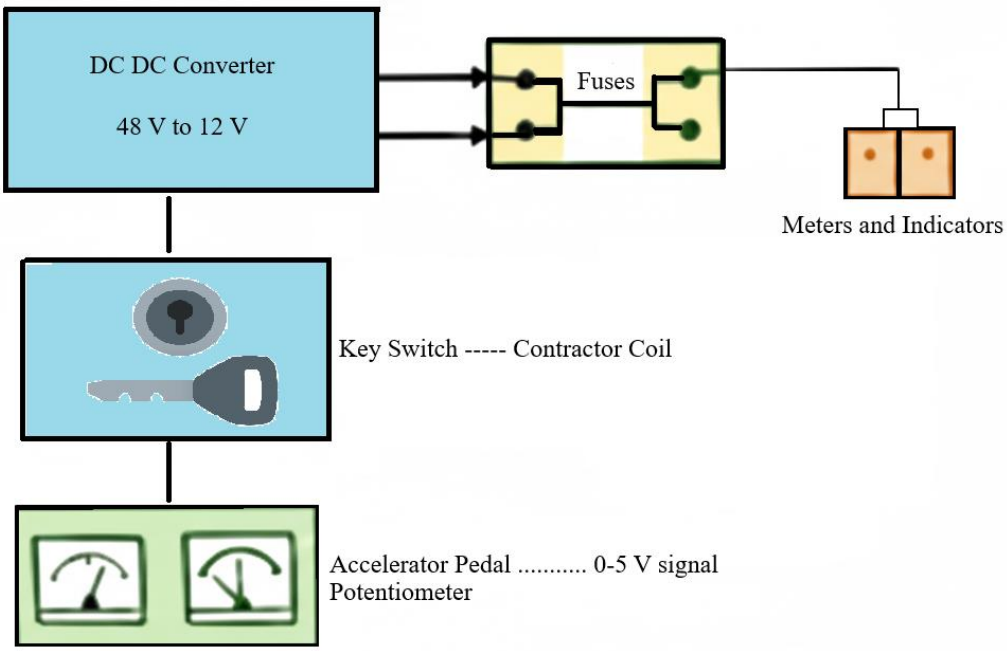

Figure 1b. Schematic of Complete Electrical Wiring of the EV with Low Voltage Control and Monitoring System.

2.2 Battery Management: LVD and LRV Protocols

In order to reduce the risk of permanent plate sulfation and deep discharge, an intelligent Battery Management System (BMS) was designed. The system has a preprogrammed loop of voltage hysteresis to maintain State of Health (SoH) of the lead-acid cells.

2.2.1 Low-Voltage Disconnect (LVD):

Upon reaching a cell voltage of 10.8 V, the RB4 pin of the MCU enables the TIP142 Darlington pair. This shuts off the G5Q-DC12 relay leaving the load unconnected to allow the cells to rest.

2.2.2 Low-Voltage Reconnect (LRV):

When charging from the solar array or AC charger restores the battery voltage to 12.5 V, the relay is re-engaged so that the system returns to normal operation. Reliability of the system is maintained with the use of Schottky diodes to avoid reverse current leakage to the PV panels nocturnally, and heavy-duty magnetic contactors are being used to switch loads more than 30 A. The LVD/LRV circuit diagram is illustrated in Figure 2.

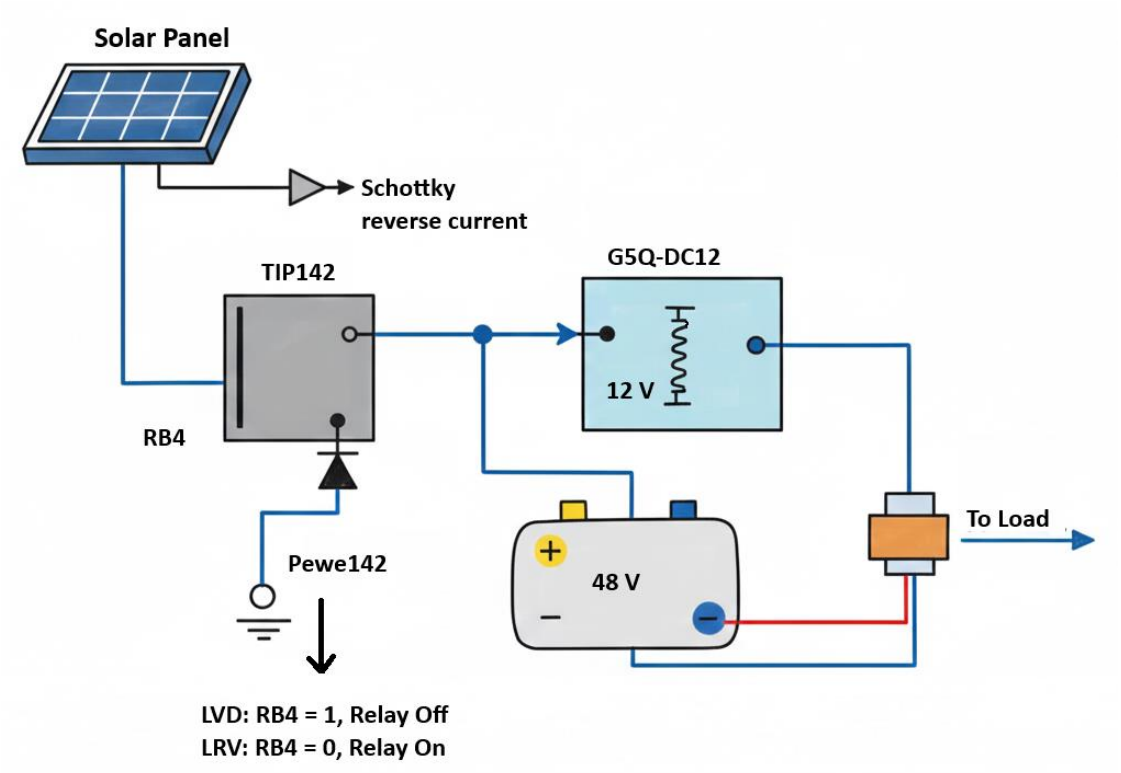

Figure 2. LVD/LRV Circuit Schematic

2.3 Propulsion Control and Drive Logic

A DC series motor has been chosen in the drivetrain because it has strong torque-speed properties. This is done by means of a Pulse Width Modulation (PWM) controller, which varies the voltage applied to the armature windings with the foot-pedal potentiometer input.

Directional control is affected through a Double Pole Double Throw (DPDT) type switching mechanism that is installed in the gearbox housing as indicated in Figure 3. Reversal of the armature winding polarity versus the field winding makes the EV smooth changes between forward and reverse conditions, eliminating the need for a complex mechanical transmission.

2.4 Power Supply and Rectifier Configuration

A high-capacity AC-DC rectification stage was designed and used in grid-tied charging and laboratory tests. A VA Variac (Auto-transformer) modifies the voltage downward to 55 V AC from the 220 V AC, which is further converted by a KBPC3510 full-bridge rectifier.

A capacitor bank of 10, 000 uF is used to reduce voltage ripple giving a stabilized DC output of 77.9 V peak.

The system provides an average charging current of 21.92 A, which has the ability to swiftly recharge the 70 Ah battery bank, and is thermally stable.

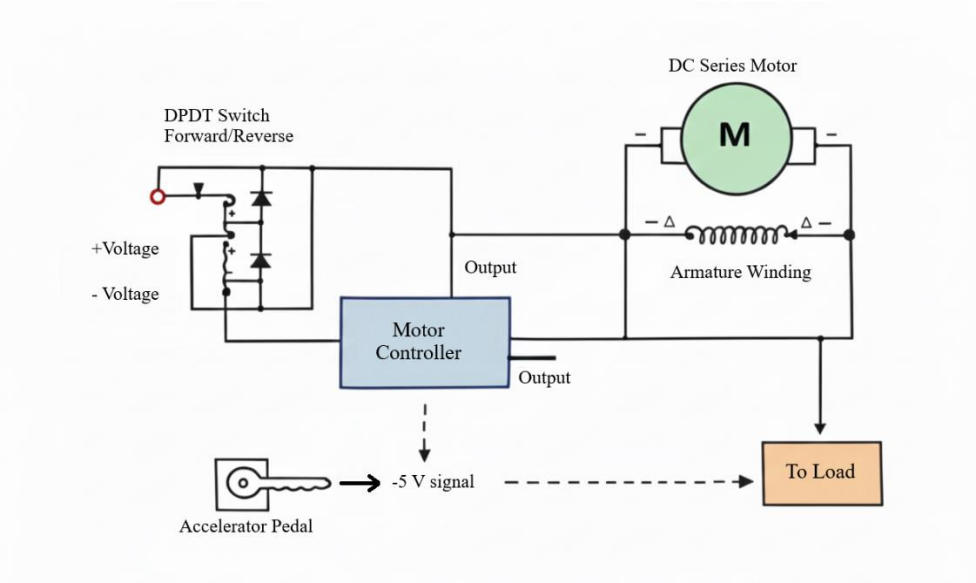

Figure 3. DC Motor and Gearbox Control Schematic

2.5 Integrated System Architecture

The complete energy flow of the SEV can be summarized using the block diagram of system architecture (Figure 4). The architecture is organized in a rational flow. A PVM charge controller regulates the energy gathered by the Solar PV array. The main energy storage system is a 48 V battery module. The throttle signals are interpreted by the motor controller that regulates the flow of power. The one horsepower motor transforms electrical power to mechanical torque and transfers it to the wheels via the built-in drive system.

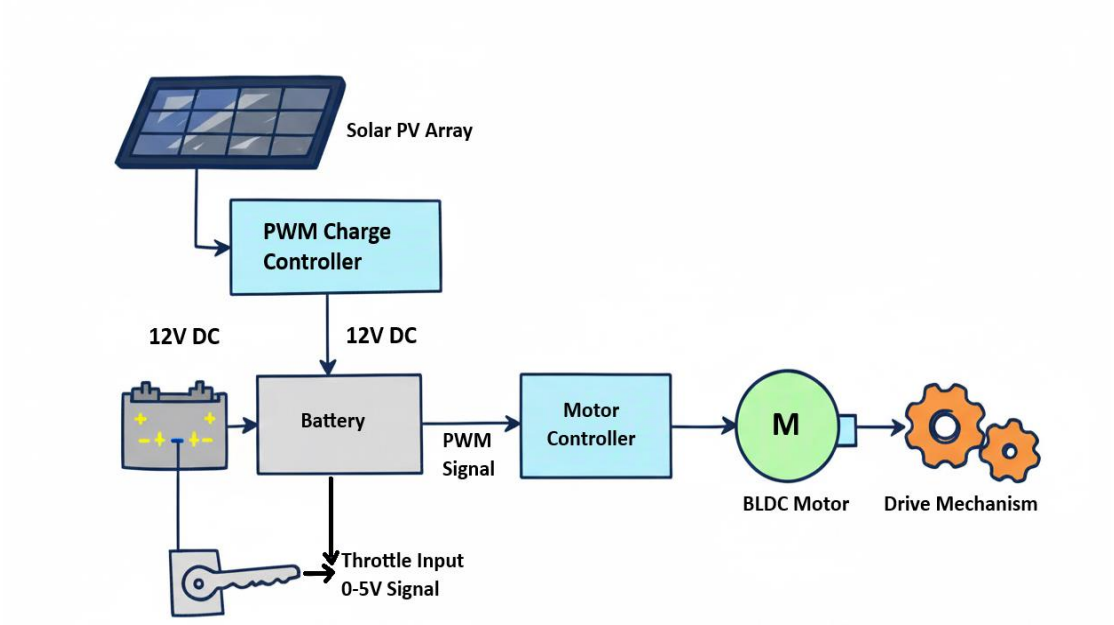

Figure 4. System Architecture of the Eco-Friendly Solar Mini Car

3. Mechanical Design and Aerodynamic Optimization

The mechanical architecture was designed to give a balance between structural rigidity and power

to weight ratio. The mechanical merging of the subsystems makes the electrical propulsion effective and steady.

3.1 Chassis and Structural Framework

The car base is made of custom-designed rolling chassis. Mild Steel Box Sections (ERW) was chosen to be used in making the frame to allow durability and at the same time lightweight profile.

3.1.1 Fabrication

The chassis was built by welding ERW pipes with a high level of precision to give high torsional stiffness to resist the stress of the 3.36 kWh battery pack and the 1 kW motor. Figure 5 shows initial chassis fabrication with rear differential and drivetrain alignment.

3.1.2 Layout

Chassis design follows a low center of gravity approach with the heavy battery bank being placed in a low centralized location, which greatly enhances cornering stability.

3.2 Vehicle Dynamics: Suspension, Steering, and Braking

The following subsystems were incorporated so as to make sure that the passengers were comfortable and able to hold the road:

3.2.1 Suspension System

The car has a four-wheel independent suspension system. It makes use of coil-over hydraulic shock absorbers and independent carbon springs to isolate the cabin to road irregularities. Such a design provides all the four wheels with optimal contact with the road surface particularly when accelerating and braking. Figure 6 shows rear suspension assembly on a custom chassis.

3.2.2 Steering Mechanism

A steering mechanism was done in manual form, which was a rack-and pinion. This option offers the driver with high steering ratio and direct feedback, which is critical to the maneuverability of small-scale urban EVs.

3.2.3 Braking System

The car also has rear drum brakes which are operated by levers. This mechanical system has a good stopping force and is maintained to be able to manage the momentum of the vehicle when at its maximum speed of 28 km/h.

3.3 Flow Control and Aerodynamic Optimization

The prototype outer body was developed to handle the boundary layer and reduce pressure drag to make the most of the 1 kW drive train. The aerodynamic profile was made sleek in order to reduce the large wake effect due to bluff-body vehicles. The overall flow diagram in Figure 6 shows the following important design characteristics and their roles.

3.3.1 Frontal Pressure Control and Flow Attachment

Figure 7(a) indicates that the flow separation is reduced by the rounded contours of all the leading edges and pillars of the A-pillars. This design supports and optimizes the Attached Body Flow, which guides incoming air to ensure streamlined flow following the contours of the windshield and roofline. A Stagnation region in the front face of the bumper forms a region of maximum local pressure (P_{high}) which is then split off by the splitter (Figure 7(c)).

3.3.2 Splitter and Air Dam Assembly

The front splitter and air dam have been added to control airflow in the nose of the vehicle (Figure 7(b)). This assembly has a major role of flow diversion instead of creating downforce force. The aerodynamic forces remain slight while running at 28 km/h, though the directed airflow boosts stability and prevents excessive unsteady separation.

The splitter puts a pressure on the upper surface which is not in motion and restricts the flow of air into the underbody space. The air dam also redirects the flow of air on the uncovered portions of the chassis. This will decrease underbody turbulence and help in a more reliable handling in low speed.

3.3.3 Wake Management and Drag Reduction
The rear geometry was redesigned in order to minimize the base drag due to a low-pressure wake.

3.3.3.1 Low-Pressure Wake Zone: This is a specific Low-Pressure Wake Zone that develops behind the car, as is pictured in Figure 7(d).

3.3.3.2 Drag Mitigation: The rear spoiler directs and controls the point of separation of this wake by making it smaller, to cause a reduction in the total pressure drag (F_D). This aerodynamic resistance is directly related to this increase in range of the vehicle to 20 km on solar power.

Figure 5. Initial Chassis Fabrication with Rear Differential and Drivetrain Alignment.

Figure 6. Rear Suspension Assembly on a Custom Chassis.

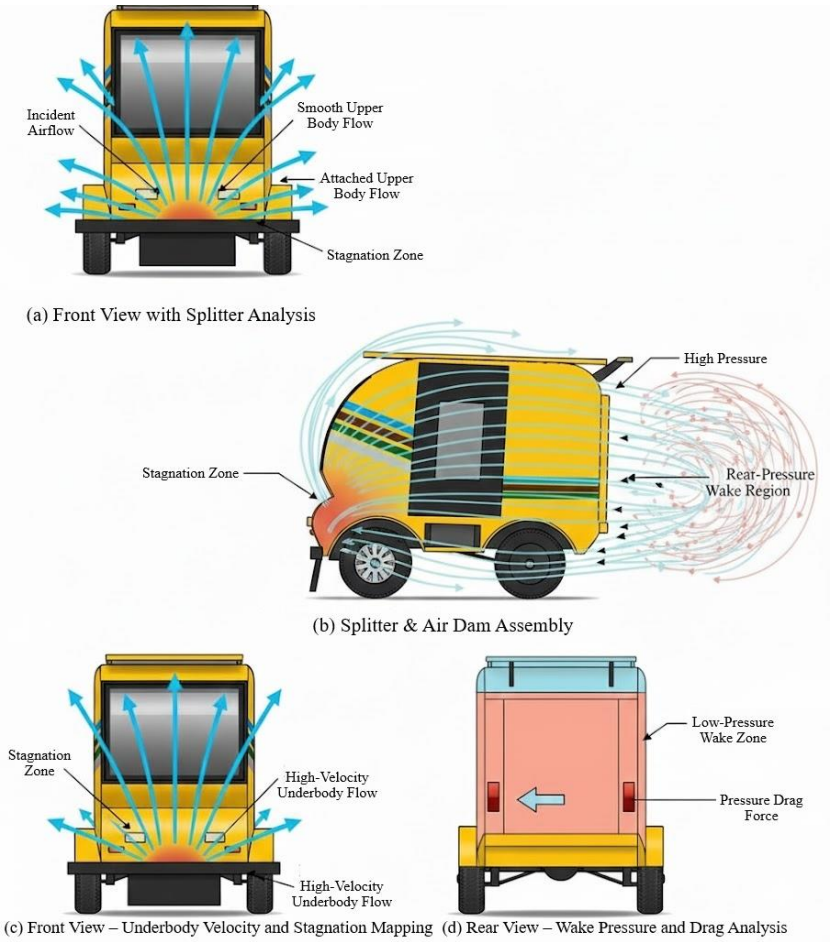

Figure 7. External Aerodynamic Configuration of the Solar Car Prototype.

3.4 Prototype Development and Assembly

The proposed design was achieved by creating a full-size working prototype. This phase was aimed at having the electrical, mechanical, and control subsystems integrated together into one functional vehicle and testing feasible constraints in the assembly.

The chassis was made out of arc welded sections of ERW mild steel. The battery packs were placed in an enclosure that is centrally positioned with a low height to ensure the center of gravity is low. The DC motor and gearbox were aligned with the rear axle to reduce the drive train losses and ease the maintenance.

The photovoltaic panels were attached to the upper body structure and were fixed at a fixed tilt. Wiring was done through insulated conduits and all the high current carrying paths were guarded or safeguarded by contactors and circuit breakers. The control unit that was installed in the sealed enclosure was made out of PIC16F876A, which is resistant to dust and vibration.

The final prototype is presented in figure 8. This prototype was the experimental basis of all the subsequent experimental measurements that were to be discussed in the following sections.

Figure 8. Completed Solar-Powered Electric Vehicle Prototype.

4. Mathematical Modeling and Performance Calculations

This section gives the analytical validation of electrical and propulsion systems. The aim is to ensure that the parameters of performance measured meet the rated parameters of the battery pack, motor, and charging system.

4.1 Electrical System Overview

Table 1 provides a summary of the important electrical components applied in the solar-powered mini car and their functional purposes. These elements characterize the electrical design of the vehicle and provide limitations on the availability of power, protection, and energy storage to be used in further calculations.

The propulsion system is entrusted to the lead-acid battery banks connected in series to supply power to a 48 V, 1 kW DC motor as indicated in Table 1. The provision of a main contactor, circuit breaker and shunt allows it to operate safely under high current conditions.

4.2 Vehicle Operating Parameters

Table 2 gives the principal electrical and operating values of the prototype. The values are used to determine the capacity of energy, the charge pattern, and the range of driving.

The battery pack is made of four 12 V, 70 Ah batteries, which are in series, giving a system voltage of 48 V. The summative of the theoretical energy storage is thus 3.36 kWh. The voltage-current ratings of the solar panel show that the photovoltaic system is an auxiliary power supply and not the main propulsion power supplier.

Table 1. Electrical System Components

Component	Specification	Function
DC Motor	48 V, 1 kW, 12 A	Propulsion
Battery Pack	4 × 12 V, 70 Ah	Energy storage
Solar Panels	78 V, 1.85 A	Supplemental charging
Charge Controller	PIC16F876A	Battery Management, PWM control
Main Contactor	30–60 A	Connect/disconnect motor from battery
Circuit Breaker	50–150 A	Overcurrent protection
Shunt	0.001 Ω	Current measurement

4.3 Energy Storage and Battery Capacity

Table 3 summarizes the electrical and energy-related computations that were performed to validate the performance of the system. These estimations are based on battery energy capacity and charging properties of which they are directly measurable in the course of experimental testing. This value is the amount of energy that can be gained in an ideal condition. In actual operation, the usable energy declines because there is depth of discharge restrictions based on the logic of the LVD and LRV protection mechanisms. The obtained values of the battery energy and the rectified peak voltage shown in Table 3 are rather close to the experimental values, which proves the electrical design consistency.

Table 2. Key Vehicle Parameters

Parameter	Value
Motor Voltage	48 V DC
Motor Power	1 kW
Motor Current	12 A
Battery Pack	4 × 12 V, 70 Ah
Total Battery Energy	3.36 kWh
Max Solar Panel Voltage	78 V
Max Solar Panel Current	1.85 A per panel
LVD	10.8 V
LRV	12.5 V

Table 3. Electrical and Energy Calculations

Parameter	Formula	Value
Torque (T)	$T \propto I$	12 A × k
Speed (ω)	$\omega \propto V$	48 V × k
Battery Energy (E)	E = V × Ah	48 V × 70 Ah = 3360 Wh
AC Rectified Peak Voltage	$V_{s(peak)} = \sqrt{2} \times V_s$	77.9 V
Average DC Charging Current	$I_{ave} = 0.62 \times I_{s(peak)}$	21.92 A

4.4 Motor Power and Electrical Consistency

The motor has a rated power of 1 kW designed for a nominal voltage of 48 V. In steady-state cruising, the current measured was about 12 A and this gives a power consumption of about 576 W. Under higher conditions of acceleration and starting conditions, the current is very high and can safely be operated by the 30 A rated motor controller.

Torque characteristics in Table 3 indicate that the motor is of series-wound type, which means that torque is highly dependent on current. It is an appropriate behavior in the case of low-speed electric cars which demand a high starting torque.

The torque and speed characteristics of the DC series motor are the normal current and voltage dependent characteristics and can thus be qualitatively than numerically modeled.

4.5 Mechanical Subsystem Summary

Table 4 lists the primary mechanical elements as well as their material choices. This table underlies the assumptions in the structural and dynamic assumptions in performance evaluation.

The installed battery mass and drives are also rigid enough to support the drive and the loads of the installed battery using an ERW mild steel chassis. The independent suspension and hydraulic shock absorbers are also used to provide stability in handling in the tested speed range.

Collectively, the tabulated data affirm the consistency of the electrical, mechanical, and control subsystems with each other and the size appropriateness of the subsystems to the planned low-speed solar-assisted operation.

Table 4. Mechanical Components

Component	Material	Description
Chassis	Mild Steel Box Section	Lightweight, stiff
Rear Axle	Steel pipe	Supports motor and rear wheels
Front Suspension	Independent, carbon springs	Road isolation, stability
Steering	Rack-and-pinion	Manual control
Shock Absorbers	Hydraulic	Absorbs vertical motion
Brakes	Drum brakes	Rear wheels, lever-actuated

5. Results and Discussion

5.1 Experimental Setup and Test Conditions

The experimental tests were done in a paved road when the sun was clear to maintain stable sunshine. Testing was done at 11.30 AM to 2.30 PM. The ambient temperature was 24 to 29 ^{0}C. It was driven by one driver and its overall cargo weight was about 120 kg, which included a set of batteries and onboard elements.

The speed of the vehicle was determined by a calibrated digital speedometer. Shunt based measurements and digital multimeters were used to measure battery voltage and current. Charging efficiency was given as the ratio of the electric energy to the battery terminals to the energy provided at the solar array and AC charging source. The tests were carried out three times, and average values are given to reduce random measurement error.

The driving range was measured by driving the vehicle at a constant speed of about 25km/h at level ground until low voltage disconnect level was achieved. Solar contribution to the power generation on-board was considered as auxiliary energy source, and not as the main propulsion.

5.2 Vehicle Speed and Power Performance

The prototype was capable of reaching a speed of 28 km per hour on flat ground. At steady state

cruising the measured current at 48 V was 12 A, which would translate to a power consumption of 576 W. This is the expected value of the motor specification and indicates that the driveshaft does not overheat or exceed the electrical limits of safety.

An increase in current draw was encountered in initial acceleration which is typical of DC series motors. The motor's control and protection modules had the ability to safely operating these transient currents. The obtained performance proves that the chosen motor and controller combination can be used in a low-speed urban environment.

5.3 Driving Range and Energy Consumption

The vehicle had a range of about 20 km with a fully charged battery pack and some assistance of the sun when in use. The solar panels would offer a small extension of reach in optimal sunshine conditions but they were not the main driving energy supply.

The rolling resistance, the drivetrain losses and the electrical inefficiencies were the dominant aspects of energy consumption during operation. The range is thus agreeable to the mass of vehicles, the capacity of the battery, and the rating of the motor power.

5.4 Charging Performance and Efficiency

The PWM based system of charging proved to be stable and reliable both in solar and AC charging. The highest efficiency in terms of charging was about 92%.

The logic of the low voltage disconnects and reconnection of the battery proved to be an effective measure that prevented deep battery discharge and re-activation under controlled conditions after battery voltage returned. This protection scheme helps to enhance better battery life and safety of operation especially on lead acid energy storage systems.

5.5 Discussion of System Level Performance

The experiment findings are indicative of internal consistency of electrical design, mechanical configuration, and performance. The realized speed and range are suitable to a low-speed solar assisted electric vehicle that is to be used over the short distance mobility. The input of the solar array can be regarded as an energy supplement and not energy autonomy.

The aerodynamic characteristics enhanced the flow stability and the vehicle handling when moving at low speed but did not affect the overall energy consumption significantly. The overall system performance ascertained that the prototype has been functioning as desired, and compliant with the design requirements of simplicity, safety, and feasible practicality.

6. Conclusion and Future Work

6.1 Conclusion

This research paper outlined the design, construction, and experimental testing of a miniature-sized solar powered electric vehicle prototype to be used in low-speed mobility. The car managed to incorporate a 1 kW DC motor, a 48 V lead acid battery pack, a PWM based charging system and a simple voltage-based battery protection scheme. The chassis, suspension, steering and braking system were all mechanical subsystems designed to facilitate stable operation at low speed.

The prototype was experimentally tested, which proved that it does not surpass the intended electrical and mechanical limits. The vehicle attained a top speed of 28 km/hour and a driving range of around 20 km with solar assistance under the given test conditions. A charging efficiency of approximately 92% has shown that there is good power regulation and good management of the battery.

The findings show that solar assisted electric vehicles can offer realistic short scale mobility provided that they are designed with realistic performance expectations. The prototype is used as an applied engineering research and educational development case study, but not a high-performance transportation solution.

6.2 Future Work

Further development may be aimed at making it more efficient, range, and system durability.

The replacement of the lead acid battery pack with lithium-based energy storage can lead to a

massive gain in energy density and cycle life. Power consumption can also be reduced by reducing the mass of the vehicle such as the use of alternative chassis materials. Regenerative braking may be incorporated to augment energy recovery under deceleration. Modern real time monitoring of battery state of charge, motor temperature, and solar input may also be used to improve system control and quality of data.

These can be used to facilitate the conversion of this prototype into a more developed low speed electric vehicle platform capable of being put through extensive testing and practical implementation.

References:

[1] A. Alishaq, D. Mehlig, A. Alishaq, and D. Mehlig, "Towards Sustainable Mobility: Assessing the Benefits and Implications of Internal Combustion Engine Vehicle Bans and Battery Electric Vehicle Uptake in Qatar," *Atmosphere*, vol. 15, no. 6, May 2024, doi: 10.3390/atmos15060677.

[2] J. S. G. Collazos, L. M. C. Ardila, and C. J. F. Cardona, "Energy transition in sustainable transport: concepts, policies, and methodologies," *Environ. Sci. Pollut. Res.*, vol. 31, no. 49, pp. 58669–58686, Oct. 2024, doi: 10.1007/s11356-024-34862-x.

[3] "Decarbonising urban transport: an overview of electric vehicles, public transport, and sustainable infrastructure in achieving net-zero emissions | Discover Global Society." Accessed: Jan. 01, 2026. [Online]. Available: https://link.springer.com/article/10.1007/s44282-025-00201-9?utm_source=chatgpt.com

[4] G. Kalghatgi, "Development of Fuel/Engine Systems—The Way Forward to Sustainable Transport," *Engineering*, vol. 5, no. 3, pp. 510–518, Jun. 2019, doi: 10.1016/j.eng.2019.01.009.

[5] R. R. Timilsina, J. Zhang, D. B. Rahut, K. Patradool, and T. Sonobe, "Global drive toward net-zero emissions and sustainability via electric vehicles: an integrative critical review," *Energy Ecol. Environ.*, vol. 10, no. 2, pp. 125–144, Apr. 2025, doi: 10.1007/s40974-024-00351-7.

[6] B. Suproń, I. Łącka, B. Suproń, and I. Łącka, "Research on the Relationship between CO2 Emissions, Road Transport, Economic Growth and Energy Consumption on the Example of the Visegrad Group Countries," *Energies*, vol. 16, no. 3, Jan. 2023, doi: 10.3390/en16031340.

[7] B. Diouf, "The electric vehicle transition," *Environ. Sci. Adv.*, vol. 3, no. 2, pp. 332–345, Feb. 2024, doi: 10.1039/D3VA00322A.

[8] D. Rimpas *et al.*, "Decarbonizing the Transportation Sector: A Review on the Role of Electric Vehicles Towards the European Green Deal for the New Emission Standards," *Air*, vol. 3, no. 2, Apr. 2025, doi: 10.3390/air3020010.

[9] A. Pamidimukkala, S. Kermanshachi, J. M. Rosenberger, and G. Hladik, "Barriers and motivators to the adoption of electric vehicles: A global review," *Green Energy Intell. Transp.*, vol. 3, no. 2, p. 100153, Apr. 2024, doi: 10.1016/j.geits.2024.100153.

[10] H. Zhang, M. Irfan, F. Ai, K. M. Al-Aiban, and S. Abbas, "Analyzing barriers to the adoption and development of electric vehicles: A roadmap towards sustainable transportation system," *Renew. Energy*, vol. 233, p. 121136, Oct. 2024, doi: 10.1016/j.renene.2024.121136.

[11] I. Diahovchenko, L. Petrichenko, I. Borzenkov, and M. Kolcun, "Application of photovoltaic panels in electric vehicles to enhance the range," *Heliyon*, vol. 8, no. 12, p. e12425, Dec. 2022, doi: 10.1016/j.heliyon.2022.e12425.

[12] B. Ogulcan Parlak and H. Ayhan Yavasoglu, "Assessment of Vehicle-Integrated Photovoltaics: A financial and environmental perspective," *Sustain. Energy Technol. Assess.*, vol. 72, p. 104042, Dec. 2024, doi: 10.1016/j.seta.2024.104042.

[13] S. Sagaria, G. Duarte, D. Neves, and P. Baptista, "Photovoltaic integrated electric vehicles: Assessment of synergies between solar energy, vehicle types and usage patterns," *J. Clean. Prod.*, vol. 348, p. 131402, May 2022, doi: 10.1016/j.jclepro.2022.131402.

[14] M. Yamaguchi *et al.*, "Topical Review for Vehicle Integrated Photovoltaics," *Energy Power Eng.*, vol. 16, no. 12, pp. 394–406, Dec. 2024, doi: 10.4236/epe.2024.1612020.

[15] A. Kaas, C. Wilke, A. Vanderbruggen, and U. A. Peuker, "Evaluating the influence of discharge depths of lithium-ion batteries on the mechanical recycling process," *J. Clean. Prod.*, vol. 486, p. 144541, Jan. 2025, doi: 10.1016/j.jclepro.2024.144541.

[16] A. Brissette, A. Hoke, J. Traube, F. Lu, and D. Maksimovic, *Study on the effect of solar irradiance intermittency mitigation on electric vehicle battery lifetime*. 2013, p. 267. doi: 10.1109/SusTech.2013.6617331.

[17] Y. Du, Z. Zhang, Z. Zuo, and Y. Wang, "Lithium battery charging optimization via multi-stage combined charging strategy in solar-powered vehicles," *J. Energy Storage*, vol. 83, p. 110716, Apr. 2024, doi: 10.1016/j.est.2024.110716.

[18] M. Nivas, R. Naidu, D. Mishra, and S. R. Salkuti, "Modeling and analysis of solar-powered electric vehicles," *Int. J. Power Electron. Drive Syst. IJPEDS*, vol. 13, p. 480, Mar. 2022, doi: 10.11591/ijpeds.v13.i1.pp480-487.

[19] Y. Oukhouya ali and J. EL Haini, "Energy management strategies for grid-integrated photovoltaic and battery energy storage systems-enhanced electric vehicle charging stations: Classical approaches and neural network solutions," *Sustain. Energy Grids Netw.*, vol. 43, p. 101926, Sep. 2025, doi: 10.1016/j.segan.2025.101926.

[20] N. V. K. Rao and K. B. Krishna, "Development of a solar-integrated energy management system for grid-to-vehicle and vehicle-to-grid power exchange," *Sci. Rep.*, vol. 15, no. 1, p. 44744, Dec. 2025, doi: 10.1038/s41598-025-28410-x.